

## Reconsidering Composite Higgs Loop Effects in the Top Mode Standard Model

Michio HASHIMOTO <sup>\*)</sup>

*Department of Physics Nagoya University, Nagoya 464-8602 Japan*

(Received April 27, 1998)

Composite Higgs loop effects in the top mode standard model are discussed by using the Miransky-Tanabashi-Yamawaki (MTY) approach based on the Schwinger-Dyson equation. The top mass is obtained as 179 GeV for the Planck scale cutoff ( $\Lambda \simeq 10^{19}$  GeV). This result is different from that of the Bardeen-Hill-Lindner (BHL) approach based on the renormalization group equation (RGE), with QCD plus Higgs loop effects included ( $m_t \simeq 205$  GeV). Detailed comparison of the MTY approach with the BHL approach is made. We derive “RGE” from the Pagels-Stokar formula by considering the infrared mass as the “renormalization point”. Then, it is found that the MTY approach including the composite Higgs loop effects is only partially equivalent to the BHL approach with QCD plus Higgs loop effects. The difference essentially results from the treatment of the composite Higgs propagator, or more precisely, of  $Z_H^{-1}$ . Our results can be summarized as  $m_t$  (Ours)  $\simeq 1/\sqrt{2}m_t$  (MTY), in contrast to  $m_t$  (BHL)  $\simeq \sqrt{2/3}m_t$  (MTY), where  $m_t$  (MTY)  $\simeq 250$  GeV is the original MTY prediction without Higgs loop effects.

### §1. Introduction

Recently, the top quark was discovered by the CDF and D0 group. Its mass was found to very large, approximately 174 GeV.<sup>1)</sup> Why is the top quark so much heavier than other quarks and leptons? The explication of this mass hierarchy is one of the most urgent and interesting problems in particle physics. Since only the top quark mass is near the electro-weak symmetry breaking scale 250 GeV, it seems natural to think that the top quark may have an intimate relation to electro-weak symmetry breaking; that is the top quark may be connected with the Higgs sector in the standard model (SM). An idea related to this thought is that concerning the top quark condensate, which was proposed by Miransky, Tanabashi and Yamawaki (MTY)<sup>2)</sup> and by Nambu,<sup>3)</sup> before experiments revealed the top quark mass to be as large as it is. In this idea, the standard Higgs scalar is replaced by the corresponding bound state of the top and anti-top quarks. Thus the model may be called the “top mode standard model” (TMSM), in contrast to the ordinary SM using the elementary

---

<sup>\*)</sup> E-mail: michioh@eken.phys.nagoya-u.ac.jp

Higgs particle, the ‘‘Higgs mode’’ standard model. While the original MTY approach to the TMSM was based on the Schwinger-Dyson (SD) equation and the Pagels-Stokar (PS) formula,<sup>4)</sup> the TMSM has been further formulated elegantly through a renormalization group (RG) approach by Bardeen, Hill and Lindner (BHL)<sup>5)</sup> using the 1-loop RG flow of the SM, in which the Higgs particle becomes composite at a scale  $\Lambda$ .<sup>6)</sup> It is known<sup>7)</sup> that the BHL approach including only QCD effects is equivalent to the MTY approach at  $1/N_c$ -leading order.

The advantage of the TMSM is to obtain the relation of the electro-weak symmetry breaking scale to the top quark mass and the Higgs particle ( $t\bar{t}$ ) mass without introducing unknown particles. In this model, however, there has been the difficulty that the top quark mass is predicted to be over 200 GeV. If we consider the ‘‘top mode GUT’’<sup>8)</sup> etc., of course, we can bring down the top quark mass.

However, we wish to consider whether or not the TMSM of the original simplest version is dead by including loop effects of the composite Higgs boson and the weak gauge boson. In the BHL approach, which is based on the perturbative RGE, it does not seem that the situation is changed, for instance, by using 2-loop RGE<sup>9)</sup> or 3-loop RGE. Thus we will take the original MTY approach. In the MTY approach, the mass function behavior at higher momentum is important. This means that the behavior of the effective top-Yukawa coupling near cutoff is described clearly. This is in contrast to the BHL approach in which the top-Yukawa in the higher momentum region is ambiguous because of a large top-Yukawa.

In this paper, we consider the SD equation including composite Higgs boson loop effects in addition to the MTY analysis. Since the composite Higgs propagator, which was obtained by Appelquist, Terning and Wijewardhana,<sup>10)</sup> includes the ladder graph of gluon, the behavior of the propagator is quite different from the usual one; i.e., the composite Higgs propagator acquires an extra momentum dependence of  $Z_H^{-1}(p^2)$  [see Eq. (3.8):  $Z_H^{-1}(p^2) \propto (\ln p^2/\Lambda_{\text{QCD}}^2)^{-1/7} - (\ln \Lambda^2/\Lambda_{\text{QCD}}^2)^{-1/7}$ ]. In addition to this extra factor, the Yukawa-type vertex  $\Gamma_s(p^2)$  also includes ladder effects [see Eq. (3.10)]. Due to the extra factor and the Yukawa-type vertex, we numerically determine the top mass to be 179 GeV for the Planck scale cutoff ( $\Lambda \simeq 10^{19}$  GeV).

Moreover, we give the “RGE” for the top-Yukawa by using the PS formula and the SD equation, and clarify the relation between the MTY approach and the BHL approach. We should mention that to combine our “RGE” with the BHLs RGE in the small top-Yukawa region is *meaningless*, because the two methods are different. Our “RGE” flow including QCD plus Higgs loop effects damps more rapidly than that in the BHLs RGE. Thus, our top-Yukawa at the quasi-IR fixed point is brought down. *The difference essentially results from the treatment of  $Z_H^{-1}$ .* In our “RGE”, the dependence of  $Z_H^{-1}(p^2, M^2)$  on the physical momentum  $p$  is different from that on the infrared mass  $M$ , which is regarded as the “renormalization point”, while there is no such a distinction for  $Z_H^{\overline{MS}}(\mu^2)$  in the  $\overline{MS}$  scheme. As a result, the answer obtained in our approach is different from that in the BHL approach. Actually, if we start with the gauged Yukawa model by applying the improved ladder calculation to the top-Yukawa vertex, we find that our “RGE” is equivalent to that of BHLs, as long as we use the solution of the 1-loop RGE as the running top-Yukawa.

This paper is organized as follows. In § 2, we briefly review the analysis of the ladder SD equation including only QCD effects, following to MTY.<sup>2), 11)</sup> Next, we consider the SD equation including the Higgs boson loop effects. Then, we introduce the non-local gauge<sup>12)</sup> so as to be consistent with the bare vertex approximation to the SD equation. In § 3, we numerically analyze the SD equation for the mass function. In § 4 we consider the relation between the MTY approach and the BHL approach. Section 5 is devoted to summary and discussions.

## §2. Non-local gauge

In this section, we consider the SD equation with one-gluon-exchange graph plus Higgs-boson-loop effects included. We introduce a non-local gauge<sup>12)</sup> so as to be consistent with the bare vertex approximation to the SD equation. In this gauge, the SD equation is reduced to a single equation for the mass function.

Before consideration of  $SU(2)_L \times U(1)_Y$  flavor symmetry corresponding to the SM, we first consider  $U(1)_L \times U(1)_R$  flavor symmetry for simplicity in the  $SU(N_c)$ -

gauged Nambu-Jona-Lasinio (GNJL) model:

$$\mathcal{L} = \bar{\psi}(i\rlap{\not{\partial}} - g\mathbf{A})\psi + \frac{G}{2N_c} \left[ (\bar{\psi}\psi)^2 + (\bar{\psi}i\gamma_5\psi)^2 \right] - \frac{1}{2}\text{tr}(F_{\mu\nu}F^{\mu\nu}), \quad (2.1)$$

$$\rightarrow \bar{\psi}(i\rlap{\not{\partial}} - g\mathbf{A})\psi - \bar{\psi}(\sigma + i\gamma_5\pi)\psi - \frac{N_c}{2G}(\sigma^2 + \pi^2) - \frac{1}{2}\text{tr}(F_{\mu\nu}F^{\mu\nu}), \quad (2.2)$$

where we have used the auxiliary field method,  $\sigma = \bar{\psi}\psi$  and  $\pi = \bar{\psi}i\gamma_5\psi$ . Here,  $\psi$  belongs to the fundamental representation of  $SU(N_c)$ , and  $g$  and  $G$  are the gauge coupling and the 4-fermi coupling, respectively.

The simplest version of the GNJL model, the  $U(1)$ -gauged NJL model with  $U(1)_L \times U(1)_R$  chiral symmetry, was first studied by Bardeen, Leung and Love in the ladder SD equation.<sup>13)</sup> A full set of spontaneous chiral symmetry breaking solutions of the ladder SD equation and the critical line were discovered by Kondo, Mino and Yamawaki, and independently by Appelquist, Soldate, Takeuchi and Wijewardhana.<sup>14)</sup> This dynamics was applied to the phenomenology, i.e., the TMSM, by Miransky, Tanabashi and Yamawaki.<sup>2)</sup>

We now give a brief review of the MTY result. We consider the SD equation for the fermion propagator  $iS_f^{-1}(p) \equiv A(-p^2)\not{p} - B(-p^2)$  with a one-gluon-exchange graph, which is obtained from the Cornwall-Jackiw-Tomboulis (CJT) potential<sup>15)</sup> of  $O(N_c)$  under a 2-loop approximation. We use the bare vertex approximation to the coupling of the fermion and gauge boson. If we take the Landau gauge, the wave function  $A(p_E^2)$  is equal to unity. Therefore, the Landau gauge is the most preferable in this approximation for consistency with the Ward-Takahashi (WT) identity.<sup>16)</sup> After angular integration in Euclidean momentum, the SD equation for the mass function takes the form

$$B(x) = \sigma + 3g^2C_2 \int \frac{dy}{(4\pi)^2} y \frac{B(y)}{y + B(y)^2} \frac{1}{\max(x,y)}, \quad (2.3)$$

where  $C_2 = (N_c^2 - 1)/2N_c$  is the quadratic Casimir constant of the fundamental representation, the chiral condensation  $\sigma$  is by definition given by  $\sigma = \frac{g}{\Lambda^2} \int dy y \frac{B(y)}{y + B(y)^2}$  with  $g = \Lambda^2 G/4\pi^2$ , and  $x \equiv p_E^2$ . Hereafter we use only Euclidean momentum and omit the subscript of  $E$ . Equation (2.3) can be rewritten as the following differential

equation and boundary conditions (BC's):

$$B''(x) - \frac{\left(\frac{\lambda(x)}{x}\right)''}{\left(\frac{\lambda(x)}{x}\right)'} B'(x) - \left(\frac{\lambda(x)}{x}\right)' \frac{x B(x)}{x + B^2} = 0, \quad (2.4)$$

$$B(\Lambda^2) + \frac{1}{1 + \frac{1}{\ln \Lambda^2 / \Lambda_{\text{QCD}}^2}} \Lambda^2 B'(\Lambda^2) = \sigma, \quad (\text{UV-BC}) \quad (2.5)$$

$$x^2 B'(x) \rightarrow 0 \quad (x \rightarrow 0), \quad (\text{IR-BC}) \quad (2.6)$$

where we have used a standard technique called the ‘‘improved ladder’’ calculation to take account of running effects of the gauge coupling in the non-Abelian gauge theory:<sup>17)</sup>

$$\lambda \equiv \frac{3C_2 \alpha_s}{4\pi} \Rightarrow \lambda(x)\theta(x-y) + \lambda(y)\theta(y-x), \quad (2.7)$$

$$\lambda(x) \equiv \frac{c_m}{\ln(x/\Lambda_{\text{QCD}}^2)}, \quad (2.8)$$

$$c_m \equiv \frac{9C_2}{11N_c - 2N_f} = 4/7 \quad (\text{for SM}). \quad (2.9)$$

From (2.4), the mass function is obtained approximately as<sup>11)</sup>

$$B(x) \simeq M \left( \frac{\ln x / \Lambda_{\text{QCD}}^2}{\ln M^2 / \Lambda_{\text{QCD}}^2} \right)^{-c_m}, \quad (2.10)$$

where  $M$  is the infrared mass defined by  $M = B(M^2)$ . The PS formulae with isospin breaking, which were obtained by MTY,<sup>2)</sup> are

$$F_{\pi^0}^2 = \frac{N_c}{8\pi^2} \int_0^{\Lambda^2} dx x \frac{B(x)^2 - \frac{x}{2} B(x) B'(x)}{(x + B(x)^2)^2}, \quad (2.11)$$

$$F_{\pi^\pm}^2 = \frac{N_c}{8\pi^2} \int_0^{\Lambda^2} dx \frac{B(x)^2 - \frac{x}{2} B(x) B'(x) + \frac{B(x)^3 B'(x)}{x + B(x)^2}}{x + B(x)^2}, \quad (2.12)$$

where we have assumed maximal isospin breaking ( $m_b = 0$ ). Even in this case,  $\delta\rho = F_{\pi^\pm}^2 / F_{\pi^0}^2 - 1$  is about 2%. From  $F_\pi = 246$  GeV, MTY predicted the top mass as 250 GeV with cutoff  $\Lambda = 10^{19}$  GeV.

Recently, the top quark was discovered and the mass was determined to be about 174 GeV, which is somewhat smaller than the MTY value, though on the order of the weak scale, as predicted by MTY. Thus, we consider the SD equation with one-gluon-exchange graph plus Higgs-loop effects (Fig. 1). The SD equation for Fig. 1 is

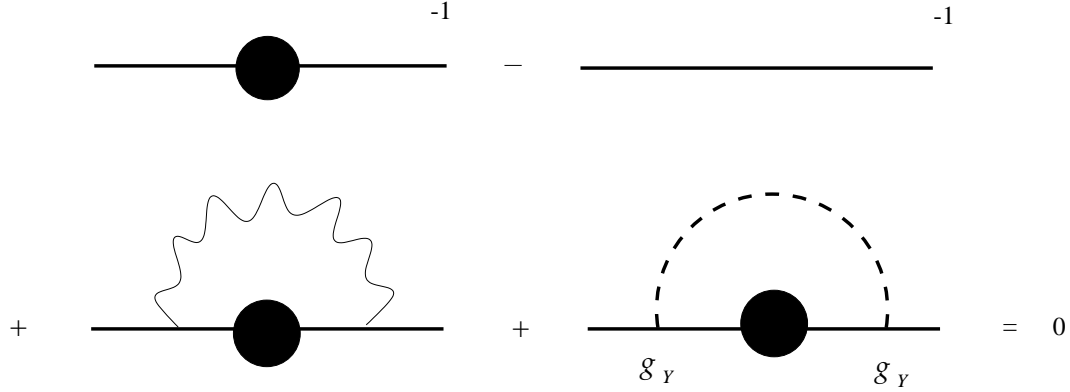


Fig. 1. The Schwinger-Dyson equation. The solid line with the shaded blob, the solid line without the shaded blob, the wavy line, and the dotted line represent the full fermion propagator  $S_f$ , the bare fermion propagator, the bare gauge boson propagator  $D_{\mu\nu}$ , and the composite Higgs propagator  $D_H$ , respectively. Note that the bare fermion propagator inverse to the momentum  $p$  is equivalent to  $\not{p} - \sigma$  in the auxiliary field method.

given as follows:

$$\begin{aligned}
A(p^2) = & 1 + \frac{g^2 C_2}{p^2} \int \frac{dk^4}{(2\pi)^4} \frac{A(k^2)}{A(k^2)^2 k^2 + B(k^2)^2} \left[ \frac{p \cdot k}{q^2} + 2 \frac{(p \cdot q)(k \cdot q)}{(q^2)^2} \right] \\
& + \frac{g^2 C_2}{p^2} \int \frac{dk^4}{(2\pi)^4} \frac{A(k^2) \xi^{-1}}{A(k^2)^2 k^2 + B(k^2)^2} \left[ \frac{p \cdot k}{q^2} - 2 \frac{(p \cdot q)(k \cdot q)}{(q^2)^2} \right] \\
& - \frac{1}{p^2} \int \frac{dk^4}{(2\pi)^4} \left[ \frac{A(k^2) p \cdot k}{A(k^2)^2 k^2 + B(k^2)^2} \sum_{\sigma, \pi} D_H(q^2) \right], \quad (2.13)
\end{aligned}$$

$$\begin{aligned}
B(p^2) = & \sigma + g^2 C_2 \int \frac{dk^4}{(2\pi)^4} \left[ (3 + \xi^{-1}) \frac{B(k^2)}{A(k^2)^2 k^2 + B(k^2)^2} \right] \\
& + \int \frac{dk^4}{(2\pi)^4} \left[ \frac{B(k^2)}{A(k^2)^2 k^2 + B(k^2)^2} (D_\sigma(q^2) - D_\pi(q^2)) \right], \quad (2.14)
\end{aligned}$$

where we have made the bare vertex approximation,  $g_Y = 1$ ,  $i\gamma_5$  for  $\sigma$ ,  $\pi$ , and  $D_{\mu\nu}(p)$  and  $D_H(p)$  are the bare gauge boson propagator ( $D_{\mu\nu}(q) = \frac{1}{q^2}(g_{\mu\nu} - (1 - \xi^{-1})\frac{q_\mu q_\nu}{q^2})$ ) and the composite Higgs propagator ( $H = \sigma, \pi$ ), respectively.

Since we take the bare vertex approximation, we need to set  $A(p^2) = 1$  for consistency with the WT identity. Of course, the coupled SD equations of the wave function and the mass function could be considered under a suitable vertex ansatz. We introduce, instead of consideration of such SD equations, the non-local gauge  $\xi^{-1}(q^2)$  so as to fix  $A(p^2) = 1$  consistently with the bare vertex approximation. From this standpoint, Eqs. (2.13) and (2.14) are reduced to a single equation for the

mass function  $B(p^2)$  by requiring  $A(p^2) = 1$  through the freedom of gauge choice.<sup>12)</sup> In this gauge,  $B(p^2)$  becomes the very mass function.

It is well known that the Landau gauge ( $\xi^{-1} = 0$ ) gives  $A(p^2) = 1$  in the analysis of the one-gluon-exchange graph; i.e., the second term and the third term in the r.h.s. of Eq. (2.13) are canceled out. We consider the following trick to reparametrize the integrating momentum:

$$0 = \int \frac{dk^4}{(2\pi)^4} \frac{1}{k^2 + B(k^2)^2} \left[ \frac{p \cdot k}{q^2} + 2 \frac{(p \cdot q)(k \cdot q)}{(q^2)^2} \right], \quad (2.15)$$

$$\simeq \int \frac{dk'^4}{(2\pi)^4} \frac{1}{q'^2 + B(q'^2)^2} \left[ \frac{p \cdot q'}{k'^2} + 2 \frac{(p \cdot k')(q' \cdot k')}{(k'^2)^2} \right], \quad (2.16)$$

where we have assumed the momentum-shift-invariant regularization and  $q(q') \equiv p - k(k')$ . By using the relation of Eq. (2.16), we can rewrite Eq. (2.13) as

$$\begin{aligned} & p^2(A(p^2) - 1) \\ = & g^2 C_2 \int \frac{dk^4}{(2\pi)^4} \frac{1}{k^2 + B(k^2)^2} \left[ -2(p \cdot q)(k \cdot q) \frac{\xi^{-1}(q^2)}{(q^2)^2} + p \cdot k \frac{\xi^{-1}(q^2)}{q^2} \right] \\ & - \sum_{\sigma, \pi} \int \frac{dk^4}{(2\pi)^4} \frac{p \cdot k}{k^2 + B(k^2)^2} D_H(q^2), \end{aligned} \quad (2.17)$$

$$\begin{aligned} \simeq & g^2 C_2 \int \frac{dk'^4}{(2\pi)^4} \frac{1}{q'^2 + B(q'^2)^2} \left[ -2(p \cdot k')(q' \cdot k') \frac{\xi^{-1}(k'^2)}{(k'^2)^2} + p \cdot q' \frac{\xi^{-1}(k'^2)}{k'^2} \right] \\ & - \sum_{\sigma, \pi} \int \frac{dk'^4}{(2\pi)^4} \frac{p \cdot q'}{q'^2 + B(q'^2)^2} D_H(k'^2), \end{aligned} \quad (2.18)$$

$$= \int \frac{y' dy' d\Omega'_k}{(4\pi)^2} \frac{p \cdot q'}{q'^2 + B(q'^2)^2} \left[ 2g^2 C_2 \frac{\xi^{-1}(y')}{y'} - \sum_{\sigma, \pi} D_H(y') \right], \quad (2.19)$$

where  $y' \equiv k'^2$  and we have set  $A(p^2) = 1$  already on the r.h.s. of Eq. (2.17). In addition, Eq. (2.18) has been obtained by shifting the integrating momentum from  $k$  to  $q'$ . We find the non-local gauge  $\xi(y)$  by setting r.h.s. to zero:

$$2g^2 C_2 \frac{\xi^{-1}(y)}{y} = \sum_{\sigma, \pi} D_H(y). \quad (2.20)$$

When we derived Eq. (2.16), we used a momentum-shift-invariant regularization, for instance, the dimensional regularization. Of course, the naive cutoff regularization is not invariant under shifting the integrating momentum. If we consider the constant mass function  $B(x) = m$  and a finite cutoff  $\Lambda$ , the r.h.s. of Eq. (2.16) is

obviously not equal to zero. Thus one might suspect whether our non-local gauge  $\xi(x)$  is consistent with  $A(x) \simeq 1$  for finite cutoff. By substituting Eq. (2.20) into Eq. (2.17), we obtain the wave function  $A(x)$  as follows:

$$x(A(x) - 1) = \int \frac{dk^4}{(2\pi)^4} \frac{1}{k^2 + B(k^2)^2} \left[ -\frac{(p \cdot q)(k \cdot q)}{q^2} - \frac{p \cdot k}{2} \right] \sum_{\sigma, \pi} D_H(q^2). \quad (2.21)$$

In the case that we take the composite Higgs propagator  $D_H(q^2)$  as the linear- $\sigma$  model type or the NJL type (see (3.2)), we can confirm  $A(x) \simeq 1$ , assuming that the scalar mass is very small compared with the cutoff  $\Lambda$ . Finally, we may consider the non-local gauge of Eq. (2.20) to be consistent with  $A(x) \simeq 1$ . If we take the naive cutoff regularization from the beginning, such a problem would not occur. In Ref. 18), the SD equations (2.13) and (2.14) are considered in the non-local gauge in such a case for the gauged Yukawa model. However, the analysis there is very complicated.

We substitute the non-local gauge of Eq. (2.20) into Eq. (2.14). Then, we obtain the integral equation for the mass function as

$$\begin{aligned} B(x) &\simeq \sigma + 3g^2 C_2 \int \frac{dk^4}{(2\pi)^4} \frac{B(k^2)}{k^2 + B(k^2)^2} \frac{1}{q^2} + \frac{1}{2} \int \frac{dk'^4}{(2\pi)^4} \frac{B(q'^2)}{q'^2 + B(q'^2)^2} \sum_{\sigma, \pi} D_H(k'^2) \\ &\quad + \int \frac{dk'^4}{(2\pi)^4} \frac{B(q'^2)}{q'^2 + B(q'^2)^2} (D_\sigma(k'^2) - D_\pi(k'^2)), \quad (2.22) \\ &\simeq \sigma + \frac{3\alpha_S C_2}{4\pi} \int dy y \frac{B(y)}{y + B(y)^2} \frac{1}{\max(x, y)} \\ &\quad + \frac{1}{32\pi^2} \int dy' y' \frac{B(y)}{y' + B(y)^2} \frac{y'}{\max(x, y')} \sum_{\sigma, \pi} D_H(y') \\ &\quad + \frac{1}{16\pi^2} \int dy' y' \frac{B(y')}{y' + B(y')^2} \frac{y'}{\max(x, y')} (D_\sigma(y') - D_\pi(y')), \quad (2.23) \end{aligned}$$

where Eq. (2.22) has been obtained by using the non-local gauge of Eq. (2.20) after shifting the integrating momentum from  $k$  to  $q'$ . Note that to derive Eq. (2.23) we have used the following trick for the angular integral:

$$\int \frac{dk^4}{(2\pi)^4} \frac{B(k^2)}{k^2 + B(k^2)^2} \frac{1}{q^2} \simeq \int \frac{dk'^4}{(2\pi)^4} \frac{B(q'^2)}{q'^2 + B(q'^2)^2} \frac{1}{k'^2}, \quad (2.24)$$

$$\text{i. e.,} \quad \int d\Omega'_k \frac{B(q'^2)}{q'^2 + B(q'^2)^2} \simeq \frac{y' B(y')}{y' + B(y')^2} \frac{1}{\max(x, y')}. \quad (2.25)$$



### §3. Numerical analysis of the Schwinger-Dyson equation including Higgs-Loop effects

In this section, we analyze Eq. (2·23) using two approaches, one in which the composite Higgs propagator is taken as the NJL type [Case I], and one in which we use the composite Higgs propagator obtained by ladder  $1/N_c$ -leading analysis<sup>10)</sup> (i.e., the NJL-type vertex at  $1/N_c$ -leading order plus the gauge-boson-ladder graph included)[Case II].

Since we are interested in the high momentum behavior of  $B(x)$ , we may neglect the Higgs mass; i.e., we assume  $D_\sigma(y') \simeq D_{\pi^0}(y')$ .

First, we take the composite Higgs propagator  $D_H(p^2)$  as the NJL model propagator [Case I] for comparison of our analysis with the BHL approach including only QCD plus Higgs loop effects. The NJL-type propagator in the high momentum region is given approximately by

$$D_H^{-1}(x) - D_H^{-1}(0) = -\frac{N_c}{8\pi^2}x \left[ \ln \left( 1 + \frac{\Lambda^2}{\sigma^2} \right) - I(x, \sigma^2) + \frac{2\Lambda^2 + 4\sigma^2 + x}{4\Lambda^2 + 4\sigma^2 + x} I(x, \sigma^2 + \Lambda^2) \right], \quad (3.1)$$

$$\simeq -\frac{N_c}{8\pi^2}x \left( -\ln \frac{x}{\Lambda^2} + r \right), \quad (3.2)$$

$$I(x, z) \equiv 2\sqrt{\frac{x+4z}{x}} \operatorname{arctanh} \sqrt{\frac{x}{x+4z}}, \quad (3.3)$$

$$r \equiv \frac{6}{\sqrt{5}} \operatorname{arctanh} \sqrt{\frac{1}{5}} \simeq 1.29123, \quad (3.4)$$

where we have neglected fermion condensation  $\sigma$  ( $x \gg \sigma$ ).

For  $SU(2)_L \times U(1)_Y$  flavor symmetry, we simply replace  $\sum_{\sigma, \pi}$  in Eq. (2·23) by  $\sum_{\sigma, \pi^0, \pi^+}$ . Of course, the fermion propagator takes the form  $iS_f^{-1}(p) = A(-p^2)\not{p} + A_5(-p^2)\gamma_5\not{p} - B(-p^2)$  under consideration of  $SU(2)_L$  symmetry. The pseudoscalar mass function  $B_5(-p^2)$  can always be rotated away by the chiral symmetry, but  $A_5(-p^2)$  cannot. We discuss this problem later. In any case, we now continue the analysis for Eq. (2·23).

By using the improved ladder calculation, the bifurcation method<sup>19)</sup>, and the PS formula, we obtain the fermion mass as 221 GeV for the cutoff  $\Lambda = 10^{19}$  GeV. We

will not describe this result in more detail, because this analysis is made in a parallel manner to the following analysis. This result is stable with respect to changes in  $r$ . If we vary  $r = 0 \sim 2$ , the mass is  $219 \sim 222$  GeV.

On the other hand, in the BHL approach with QCD plus Higgs loop effects (without  $SU(2)_L \times U(1)_Y$  gauge loop effects), the top-Yukawa is obtained as

$$Y(t) \equiv \frac{1}{y_t^2} = \frac{N_c + \frac{3}{2}}{16\pi^2} \frac{1}{2c_m - 1} \left( t(\mu^2) - t^{2c_m}(\mu^2)t^{1-2c_m}(\Lambda^2) \right), \quad (3.5)$$

where  $t(\mu^2) \equiv \ln \mu^2 / \Lambda_{\text{QCD}}^2$ . This top-Yukawa yields a top mass of 205 GeV. Thus, it seems that the MTY approach including the loop effects of the NJL-type propagator is *not* equivalent to the BHL approach. In next section, we will discuss the relation in detail.

Next, we consider [Case II], using the composite Higgs propagator obtained by Appelquist, Terning and Wijewardhana,<sup>10)</sup> (see Fig. 2). In the improved ladder calculation of  $1/N_c$ -leading analysis, we find

$$D_H^{-1}(x) - D_H^{-1}(0) \simeq \frac{N_c}{8\pi^2} \int_0^{\Lambda^2} dy \Gamma_s^2(y) \left[ \left( \frac{y}{x} - 2 \right) \theta(x-y) - \frac{x}{y} \theta(y-x) \right], \quad (3.6)$$

$$= -\frac{N_c}{8\pi^2} x \frac{t(\Lambda^2)^{2c_m}}{2c_m - 1} \left[ \int_0^{t(x)-t(M^2)} \frac{2(t-u)^{1-2c_m} e^{-u} (1-e^{-u})}{2} du - t(\Lambda^2)^{1-2c_m} \right. \\ \left. - t(M^2)^{1-2c_m} \left( \frac{2M^2}{x} - \frac{M^4}{x^2} \right) \right] + \frac{N_c}{8\pi^2} \int_0^{M^2} dy \Gamma_s^2(y) \left( \frac{y}{x} - 2 \right), \quad (3.7)$$

$$\simeq -\frac{N_c}{8\pi^2} x \frac{t(\Lambda^2)^{2c_m}}{2c_m - 1} \left( t(x)^{1-2c_m} - t(\Lambda^2)^{1-2c_m} \right), \quad (x \gg M^2) \quad (3.8)$$

$$t(x) = \ln x / \Lambda_{\text{QCD}}^2, \quad (3.9)$$

$$\Gamma_s(x) \equiv \frac{dB(x)}{d\sigma}, \quad (\text{The Yukawa-type vertex at zero momentum transfer}) \quad (3.10)$$

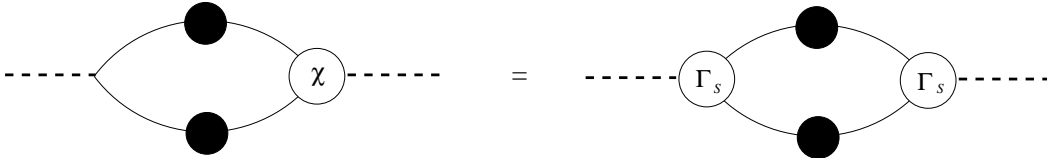


Fig. 2. The composite Higgs propagator inverse including the Yukawa-type vertex  $\Gamma_s$ . The solid line with the shaded blob, the dotted line,  $\chi$ , and  $\Gamma_s$  represent the full fermion propagator, the composite Higgs, Bethe-Salpeter amplitude, and the Yukawa-type vertex at zero momentum transfer, respectively.

$$\simeq \left( \frac{t(x)}{t(\Lambda^2)} \right)^{-c_m}, \quad (x > M^2) \quad (3.11)$$

where  $M$  is the infrared mass to normalize the mass function, and we have neglected the third, fourth and fifth terms of Eq. (3.7), because these terms are  $O(M^2) \ll x$ .

Moreover, in the present case we need to modify Eq. (2.23). If we start with the CJT potential of Fig. 3, we find that the two  $g_Y$ 's of Fig. 1 must be replaced by  $\Gamma_s$  (see Fig. 4). We can confirm this easily by differentiating the CJT potential with respect to the full fermion propagator  $S_f$ , noting that the composite Higgs propagator in Case II consists of the ladder graph (Fig. 2). Because we consider the composite Higgs propagator inverse as the r.h.s. of Fig. 2, which includes two Yukawa-type vertices of  $\Gamma_s$  in our approximation, the SD equation does not take the usual form with one bare vertex and one 1PI full-vertex. Instead, it takes the form of Fig. 4 with two Yukawa-type vertices of  $\Gamma_s$ . Finally, we obtain the SD equation for the mass function as

$$B(x) \simeq \sigma + \int dy y \frac{B(y)}{y + B(y)^2} \left[ \frac{\lambda(x)}{x} \theta(x - y) + \frac{\lambda(y)}{y} \theta(y - x) \right] + \frac{1}{32\pi^2} \int dy y \frac{B(y)}{y + B(y)^2} \frac{y\Gamma_s(x)\Gamma_s(y)}{\max(x, y)} \sum_{\sigma, \pi^0, \pi^+} D_H(y). \quad (3.12)$$

In this expression, the divergence of  $t(\Lambda^2)^{2c_m}$  from  $D_H^{-1}(y)$  is canceled out by the same one from the two  $\Gamma_s$ , and the result does not depend on whether we use the expression of  $\Gamma_s(x)^2$  or  $\Gamma_s(y)^2$  in place of  $\Gamma_s(x)\Gamma_s(y)$  in Eq. (3.12). The differences between the top mass predictions are about 1 GeV in these cases.

We can solve Eq. (3.12) simply by using the bifurcation method. Then we can show that the linearized differential equation corresponding to Eq. (3.12) is not

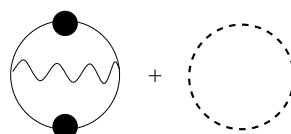
$$\Gamma_{CJT} = -iN_c \text{Tr} \text{Ln} S_f^{-1} - iN_c \text{Tr} S_f S_0^{-1} - \frac{N_c}{2G} \int dx^4 (\sigma^2 + \pi^2) + \text{diagram} + \text{diagram}$$


Fig. 3. The CJT potential. The solid line with the shaded blob, the dotted line, and the wavy line represent the full fermion propagator  $S_f$ , the composite Higgs propagator, and the bare gauge boson propagator, respectively. In the second term,  $S_0^{-1} = \not{p} - \sigma$  is the bare fermion propagator. The last term in this potential is  $O(N_c^0)$ , and the other terms are  $O(N_c)$ . Note that the composite Higgs propagator is given by Fig. 2.

second order but third order:

$$\begin{aligned} & \frac{d^3}{dt^3} B(t) + \frac{\Delta_2}{\Delta_1} \frac{d^2}{dt^2} B(t) + \left[ \frac{\Delta_3}{\Delta_1} + c_m \left( \frac{1}{t} + \frac{1}{t^2} \right) - \frac{3}{4N_c} \left( 1 + \frac{c_m}{t} \right) \frac{t^{-2c_m}}{K(t)} \right] \frac{d}{dt} B(t) \\ & + \left[ \frac{\Delta_4}{\Delta_1} \frac{c_m}{t} - \frac{3}{4N_c} \left( \frac{\Delta_5}{\Delta_1} - \frac{c_m}{t} - \frac{c_m^2}{t^2} \right) \frac{t^{-2c_m}}{K(t)} + \frac{3}{4N_c} \left( 1 + \frac{c_m}{t} \right) \frac{K'(t)}{K(t)} \frac{t^{-2c_m}}{K(t)} \right] B(t) \\ & = 0, \end{aligned} \quad (3.13)$$

$$\Delta_1 \equiv 1 + \frac{c_m + 2}{t} + \frac{c_m}{t^2}, \quad (3.14)$$

$$\Delta_2 \equiv 2 + \frac{3c_m + 6}{t} + \frac{c_m^2 + 7c_m + 6}{t^2} + \frac{c_m^2 + 4c_m}{t^3}, \quad (3.15)$$

$$\Delta_3 \equiv 1 + \frac{4c_m + 4}{t} + \frac{2c_m^2 - 13c_m + 6}{t^2} + \frac{2c_m^2 + 8c_m + 18}{t^3} + \frac{2c_m^2 + 2c_m}{t^4}, \quad (3.16)$$

$$\Delta_4 \equiv 1 + \frac{2c_m + 3}{t} + \frac{c_m^2 + 6c_m + 2}{t^2} + \frac{2c_m^2 + 4c_m - 2}{t^3} + \frac{c_m^2}{t^4}, \quad (3.17)$$

$$\Delta_5 \equiv 1 - \frac{4c_m - 7}{t} - \frac{c_m^2 + 4c_m - 6}{t^2} - \frac{c_m^3 + 2c_m^2 - 2c_m}{t^3} - \frac{c_m^3 - 2c_m^2}{t^4}, \quad (3.18)$$

$$K(t) \equiv \frac{1}{2c_m - 1} \left( t^{1-2c_m}(x) - t^{1-2c_m}(\Lambda^2) \right), \quad (3.19)$$

$$B(t) \rightarrow M, \quad (t \rightarrow t(M^2) = \ln M^2/\Lambda_{\text{QCD}}^2), \quad (3.20)$$

$$B'(t) \rightarrow 0, \quad (t \rightarrow t(M^2) = \ln M^2/\Lambda_{\text{QCD}}^2), \quad (3.21)$$

$$B''(t) \rightarrow 0, \quad (t \rightarrow t(M^2) = \ln M^2/\Lambda_{\text{QCD}}^2), \quad (3.22)$$

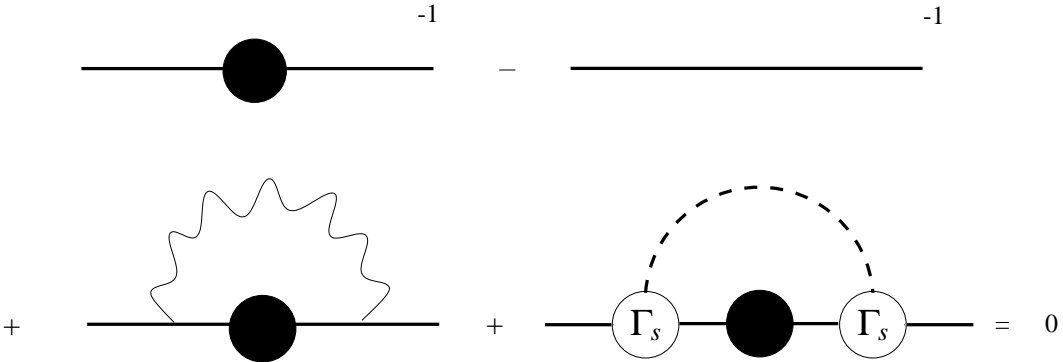


Fig. 4. The Schwinger-Dyson equation including the composite Higgs loop effects. The solid line with the shaded blob, the solid line without the shaded blob, the dotted line, and the wavy line represent the full fermion propagator, the bare fermion propagator, the composite Higgs propagator, and the bare gauge boson propagator, respectively. Note that two  $\Gamma_s$  vertices are used instead of one bare vertex and one 1PI-full vertex, because the composite Higgs propagator is given approximately by the r.h.s. of Fig. 2.

$$B'''(t) \rightarrow 0, \quad (t \rightarrow t(M^2) = \ln M^2/\Lambda_{\text{QCD}}^2). \quad (3.23)$$

By using the analytical expression of the PS formula,<sup>20)</sup> which neglects  $B'(x)$  and replaces the denominator  $x + B(x)^2$  by  $x$  in Eqs. (2.11) and (2.12),

$$F_\pi^2 = \frac{N_c}{8\pi^2} \int_{M^2}^{\Lambda^2} dx \frac{B(x)^2}{x}, \quad (3.24)$$

we numerically obtained the top quark mass  $m_t = 179$  GeV with  $\Lambda = 10^{19}$  GeV and  $F_\pi = 246$  GeV. We obtain the Table I for various cutoffs.

The differential equation Eq. (3.13) is complicated, however; the main term comes from  $\Gamma_s(x)^2 Z_H(x)$  in Eq. (3.12), where we define  $D_H^{-1}(x) \equiv -Z_H^{-1}(x)(x + M_H^2(x))$ , with  $Z_H^{-1}(x)$  being given from Eq. (3.8):

$$Z_H^{-1}(x) \simeq \frac{N_c}{8\pi^2} \frac{(\ln \Lambda^2/\Lambda_{\text{QCD}}^2)^{2c_m}}{2c_m - 1} \left( (\ln x/\Lambda_{\text{QCD}}^2)^{1-2c_m} - (\ln \Lambda^2/\Lambda_{\text{QCD}}^2)^{1-2c_m} \right). \quad (3.25)$$

This factor of  $\Gamma_s(x)^2 Z_H(x)$  blows up more rapidly than the one in Case I. Thus, the mass function in Case II grows more in the high momentum region than that in Case I, and as a result the prediction for the top mass is smaller. In the next section, the relation between the MTY approach and the BHL approach is described in detail.

$\Lambda$	$10^{21}$	$10^{20}$	$10^{19}$	$10^{18}$	$10^{17}$	$10^{16}$	$10^{15}$	$10^{14}$
$m_t$	175	177	179	181	184	187	190	194

Table I. The top mass for various cutoffs (GeV) in Case II.

#### §4. The Relation between the Miransky-Tanabashi-Yamawaki approach and the Bardeen-Hill-Lindner approach

Now we consider the relation between the MTY approach and the BHL approach. In the previous section, we found numerically that our approach is *not* precisely equivalent to the BHL approach in two cases for  $D_H(p^2)$ . Thus, we wish to obtain an analytical relation. From the bifurcation method and the analytical PS formula,

we find generally

$$F_\pi^2(M^2) = \frac{N_c}{8\pi^2} \int_{M^2}^{\Lambda^2} dx M^2 \frac{f(x)^2}{f(M^2)^2}, \quad (4.1)$$

where  $f(x)$  is a dominant solution to the SD equation for the mass function and  $B(x) = Mf(x)/f(M^2)$ . Needless to say, the mass function cannot be divided into a one variable function like  $f(x)$  under consideration of sub-dominant solutions. In fact, the mass function becomes  $B(x) = Mf(x, M^2)$  in this case, where  $f(M^2, M^2) = 1$ . In the analysis of the one-gluon-exchange graph, for instance,  $f(x)$  is nearly equal to  $(\ln x/\Lambda_{\text{QCD}}^2)^{-c_m}$  from Eq. (2.10). If we read  $M$  as a ‘‘renormalization point’’  $\tilde{\mu}$  in Eq. (4.1), we can define a ‘‘Yukawa coupling’’ corresponding to the BHL approach as <sup>7)</sup>

$$Y(\tilde{\mu}) = 1/y_t^2 \equiv \frac{F_\pi^2(\tilde{\mu}^2)}{2\tilde{\mu}^2} = \frac{N_c}{16\pi^2} \int_{\tilde{\mu}^2}^{\Lambda^2} dx \frac{f(x)^2}{f(\tilde{\mu}^2)^2}. \quad (4.2)$$

From Eq. (4.2), we obtain an ‘‘RGE’’ for the ‘‘Yukawa coupling’’ in the MTY approach as follows:

$$[\text{‘‘RGE}_{\text{MTY}}\text{’’}] \quad \frac{dY}{d\tilde{t}} = -\frac{N_c}{16\pi^2} - \frac{2f'(\tilde{t})}{f(\tilde{t})} Y, \quad \tilde{t} \equiv \ln \tilde{\mu}^2. \quad (4.3)$$

We should mention that  $Y$  becomes justly zero when  $\tilde{\mu} \rightarrow \Lambda$  in Eq. (4.2). This corresponds to the compositeness condition of the BHL approach. On the other hand, we know the 1-loop RGE of the SM for Yukawa coupling,

$$[\text{RGE}_{\text{BHL}}] \quad \frac{dY}{dt} = -\frac{N_c + 3/2}{16\pi^2} + \frac{1}{4\pi} \left( 3\frac{N_c^2 - 1}{N_c} \alpha_s + 9/4\alpha_2 + 17/12\alpha_1 \right) Y, \quad (4.4)$$

where  $t = t(\mu^2) = \ln \mu^2$ ,  $\mu$  is the renormalization point in the  $\overline{\text{MS}}$  scheme, the Higgs loop effects give the factor 3/2, and  $\alpha_1$  and  $\alpha_2$  are  $U(1)_Y$ - and  $SU(2)_L$ -gauge couplings, respectively. In the case of  $U(1)_L \times U(1)_R$  flavor symmetry, i.e., Eq. (2.2), the 1-loop RGE is given by

$$[\text{RGE}_{U(1)_L \times U(1)_R}] \quad \frac{dY}{dt} = -\frac{N_c + 1}{16\pi^2} + \frac{1}{4\pi} \left( 3\frac{N_c^2 - 1}{N_c} \alpha_s \right) Y. \quad (4.5)$$

‘‘RGE<sub>MTY</sub>’’ is similar to RGE<sub>BHL</sub> or RGE<sub>U(1)<sub>L</sub> × U(1)<sub>R</sub></sub>, and in the fact they become identical in the large  $N_c$  limit.<sup>7)</sup> However, their meanings are different. In RGE<sub>BHL</sub>, because of using a perturbative RGE, the flow of large  $y_t$  in the high energy region is

ambiguous. On the other hand, the mass function  $f(t)$  in “RGE<sub>MTY</sub>” is given clearly at higher momentum rather than at low energy. In other words, “RGE<sub>MTY</sub>” is more reliable than RGE<sub>BHL</sub> in the large  $y_t$  region. We may understand “RGE<sub>MTY</sub>” as a “non-perturbative RGE” in a sense. We should not mix the two approaches; for instance, we should not combine “RGE<sub>MTY</sub>” with RGE<sub>BHL</sub> in the small top-Yukawa region, because these approaches are based on different manners of thinking.

The differential equation for  $f(x)$  obtained from Eq. (3·12) is given approximately as follows:

$$\frac{d^2 f}{dt^2} + \frac{df}{dt} + \left( \lambda(t) - \frac{3}{4} \frac{2c_m - 1}{N_c} \frac{1}{t - t^{2c_m} t (\Lambda^2)^{1-2c_m}} \right) f = 0. \quad (4.6)$$

For Eq. (4·6), it can be shown numerically that  $f''$  is almost irrelevant. We may regard  $t(x)$  as  $\tilde{t} = t(\tilde{\mu}^2)$ , because  $f(x)$  is a one-variable function. Thus, “RGE<sub>MTY</sub>” in Case II becomes

[“RGE<sub>MTY</sub>” in Case II]

$$\frac{dY}{d\tilde{t}} = -\frac{N_c}{16\pi^2} + \left( 2\lambda(\tilde{t}) - \frac{3}{2} \frac{2c_m - 1}{N_c} \frac{1}{\tilde{t} - \tilde{t}^{2c_m} t (\Lambda^2)^{1-2c_m}} \right) Y. \quad (4.7)$$

In the same way, by use of the NJL-type propagator (3·2), “RGE<sub>MTY</sub>” in Case I can be found as

[“RGE<sub>MTY</sub>” in Case I]

$$\frac{dY}{d\tilde{t}} = -\frac{N_c}{16\pi^2} + \left( 2\lambda(\tilde{t}) - \frac{3}{2N_c} \frac{1}{-\tilde{t} + \ln \Lambda^2 / \Lambda_{\text{QCD}}^2 + r} \right) Y. \quad (4.8)$$

To be general, we obtain “RGE<sub>MTY</sub>” with QCD plus the composite Higgs loop effects [Case III] from Eq. (3·12) by using  $\Gamma_s(x)^2 Z_H(x)$  as follows:

[“RGE<sub>MTY</sub>” in Case III (the general case)]

$$\frac{dY}{d\tilde{t}} = -\frac{N_c}{16\pi^2} + 2 \left( \lambda(\tilde{t}) - \frac{1}{32\pi^2} \sum_H \Gamma_s(\tilde{t})^2 Z_H(\tilde{t}) \right) Y, \quad (4.9)$$

where we have assumed that  $f''$  is negligible. Note that Eq. (4·9) takes the same form even if we consider  $U(1)_L \times U(1)_R$  flavor symmetry, which is discussed in § 2: The term of  $\Gamma_s(x)^2 Z_H(x)$  is the same as the above one for  $H = \sigma, \pi^0$ .

If we start with the gauged Yukawa model using the improved ladder calculation to take account of the running effects of the top-Yukawa, we come to substitute  $Z_H(\tilde{t})\Gamma_s(\tilde{t})^2 = y_t^{\text{sol}}(\tilde{t})^2/2$  into Eq. (4.9), where  $y_t^{\text{sol}}$  is the solution of the 1-loop RGE. Then, we find that Eq. (4.9) in this case is just equal to  $\text{RGE}_{\text{BHL}}$  up to  $SU(2)_L \times U(1)_Y$  gauge contributions.

In our model, however,  $y_t(x)^2$  is not necessarily equal to  $\tilde{y}_t(x)^2 \equiv 2Z_H(x)\Gamma_s(x)^2$ , where the factor of 2 arises from our normalization. By definition,  $y_t(x)$  is the top-Yukawa at zero momentum transfer, while  $\tilde{y}_t(x)$  can be interpreted as the top-Higgs coupling at the same momentum of the Higgs boson as that of the top quark. Thus, these physical meanings are different. We should mention

$$F_{\pi^a}^2 = Z_{\pi^a}^{-1}(0, M^2)\sigma^2, \quad (a = 0, \pm) \quad (4.10)$$

which is derived from the WT identity for the axial-vector vertex including the auxiliary field.<sup>21)</sup> In Eq. (4.10), we have written explicitly the infrared mass dependence of  $Z_{\pi^a}$ . Hereafter, we do not distinguish  $\pi^a$ , because we have neglected the deviation of  $F_{\pi^0}$  from  $F_{\pi^\pm}$  in this paper. By the definition (4.2), another expression for our  $y_t$  is obtained as follows:

$$y_t(M^2)^2 \equiv Z_\pi(0, M^2)\frac{2M^2}{\sigma^2}, \quad (4.11)$$

$$\simeq 2Z_\pi(0, M^2)\frac{f(M^2)^2}{f(\Lambda^2)^2}, \quad (4.12)$$

where Eq. (4.12) was derived from UV-BC of  $\sigma \simeq B(\Lambda^2)$  for the mass function. On the other hand, we find

$$\tilde{y}_t(x)^2 \equiv 2\Gamma_s(x, M^2)^2 Z_H(x, M^2), \quad (4.13)$$

$$\simeq 2Z_\pi(x, 0)\frac{f(x)^2}{f(\Lambda^2)^2}, \quad (4.14)$$

where we have neglected the  $M^2$  dependence of  $Z_H$  in the high-energy region, and we have used  $Z_H(x, 0) = Z_\pi(x, 0)$  [ $H = \sigma, \pi$ ] due to the chiral symmetry. Thus, the deviation of  $\tilde{y}_t$  from  $y_t$  results essentially from that of  $Z_\pi(M^2, 0)$  from  $Z_\pi(0, M^2)$ . Of course, we cannot estimate  $Z_\pi(0, M^2)$ , as long as the bifurcation method is used. Generally speaking, it is very difficult to obtain the behavior of the mass function



around zero momentum under consideration of the running coupling effects in the SD approach.

In contrast to this, there is no such a distinction for  $Z_H^{\overline{MS}}(\mu^2)$  in the  $\overline{MS}$  scheme. This is the reason why  $\tilde{y}_t(\mu^2)$  becomes equivalent to  $y_t(\mu^2)$  in the  $\overline{MS}$  scheme. We should mention that *this point is not an artifact of the  $1/N_c$ -expansion*. The same conclusion can be also be drawn for the case of  $U(1)_L \times U(1)_R$  flavor symmetry, where  $A_5(x)$  disappears. Thus, we find that the difference between

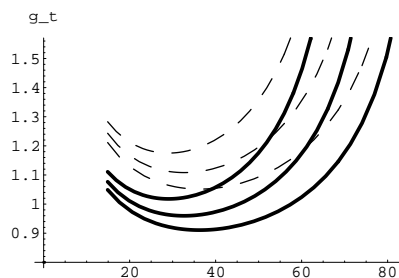


Fig. 5. The RGE flow. The dotted line and the solid line represent the BHL approach and our approach in Case II, respectively. From top to bottom,  $\Lambda = 10^{15}, 10^{17}$  and  $10^{19}$  GeV.

our result and that of the BHL is not due to the ambiguity of  $A_5(x)$ .

Actually, our result of Eq. (4.7) is different from that of BHL. Due to this difference, the RGE flow is changed (see Fig. 5).

Finally, we obtain analytical expressions of the decay constant in our approach as follows:

$$F_\pi^2(M^2) = \frac{N_c}{8\pi^2} M^2 t(M^2)^{2c_m} (-\ln M^2/\Lambda^2 + r)^{1/2} \times \int_{t(M^2)}^{t(\Lambda^2)} t^{-2c_m} (-t + \ln \Lambda^2/\Lambda_{\text{QCD}}^2 + r)^{-1/2}, \quad [\text{Ours in Case I}] \quad (4.15)$$

$$F_\pi^2(M^2) = \frac{\eta N_c}{8\pi^2} \frac{M^2}{2c_m - 1} \left[ t(M^2) - t(M^2)^{2c_m} t(\Lambda^2)^{1-2c_m} \right], \quad (4.16)$$

$$\text{where } \eta = \begin{cases} 1, & [\text{MTY/BHL including only QCD effects}] \\ \frac{3}{2}, & [\text{BHL including QCD plus Higgs loops effects}] \\ 2, & [\text{Ours in Case II}] \end{cases} \quad (4.17)$$

for  $N_c = 3$ . The analytical expressions of  $F_\pi$  in Eqs. (4.16) and (4.17) give  $m_t$  (Ours)

$\simeq 1/\sqrt{2}m_t$  (MTY) and  $m_t$  (BHL)  $\simeq \sqrt{2/3}m_t$  (MTY), where  $m_t$  (MTY)  $\simeq 250$  GeV stands for the original MTY value, corresponding to  $\eta = 1$  in Eq. (4.17).

Now, we comment on the technique of  $1/N_c$ -sub-leading analysis, because the  $1/N_c$ -expansion is partially used in our approach.

We have to notice that the mass function  $B(x)$  must not be written naively as a series in  $1/N_c$ .<sup>22)</sup> Actually, one might be tempted to expand the mass function  $B(x)$  as  $B(x) = B_0(x) + \frac{1}{N_c}B_1(x) + \dots$ . Then, one would have  $B_0(x) = -\frac{1}{N_c}B_1(x)$  on a critical line in the second order phase transition. For consistency, we would find  $B_0(x) = B_1(x) = 0$  on the critical line. Then, the critical coupling would not be changed by including any higher order  $1/N_c$ -corrections. Of course, we disagree with this claim. \*) This means that  $1/N_c$ -expansion of the order parameter should not be done naively. In Ref. 22), this point will be discussed in detail.

## §5. Summary and discussions

We have found that the top quark mass can be brought down below 200 GeV (in our analysis (Case II) 179 GeV for Planck scale cutoff), by using the SD equation with QCD plus the composite Higgs loop effects. This can be understood analytically as  $m_t$  (Ours)  $\simeq \frac{1}{\sqrt{2}}m_t$  (MTY). It was suggested that the difference of the result between our approach and the BHL approach reflects the different treatment of  $Z_H^{-1}$ . We should note that the top mass is increased by about 10% when  $SU(2)_L \times U(1)_Y$ -gauge loop effects are switched.

However, it must be mentioned that the composite Higgs propagator (3.8) may be ambiguous at higher momentum because the technique in Ref. 10) is based on resummation of the Taylor series around zero momentum of the Higgs boson. Recently, the composite Higgs boson propagator was obtained analytically under some assumptions without use of the resummation technique.<sup>24)</sup> The expression for this propagator was obtained only in the case of constant gauge coupling. In that work, the coefficient of  $(x/\Lambda^2)^{\frac{-1+\sqrt{1-4\lambda}}{2}}$  in the composite Higgs propagator is smaller than that of Ref. 10). If the situation is the same in the case of the improved ladder

---

\*) However, such an expansion of the chiral condensation  $\sigma$  is considered in Ref. 23).

analysis, the top mass may be brought down more.

Of course, some difficulties may be pointed out technically to our approach at sight. In particular, as in the previous discussion, we need to take the fermion propagator  $iS_f^{-1}(p) = A(-p^2)\not{p} + A_5(-p^2)\gamma_5\not{p} - B(-p^2)$  with consideration of  $SU(2)_L$  symmetry. This problem seems to be serious. It is expected that  $A_5(-p^2)$  can vanish if we choose a good non-local gauge for the  $SU(2)_L$  gauge. Then, we will be able to make a full analysis for the TMSM in the MTY approach. That is a future work.

### Acknowledgements

The author is very grateful to K. Yamawaki for helpful discussions and reading the manuscript. Thanks are also due to K.-I. Kondo and M. Tanabashi for providing an unpublished note<sup>18)</sup> and due to M. Lindner for discussions.

### References

- 1) Particle Data Group, Eur. Phys. J. **C3** (1998), 1.  
F. Abe et al., Phys. Rev. Lett. **80** (1998), 2767.
- 2) V. A. Miransky, M. Tanabashi and K. Yamawaki, Phys. Lett. **B221** (1989), 177; Mod. Phys. Lett. **A4** (1989), 1043.
- 3) Y. Nambu, Enrico Fermi Institute Report No. 89-08, 1989 (unpublished); in *Proceedings of the 1989 Workshop on Dynamical Symmetry Breaking*, ed. T. Muta and K. Yamawaki (Nagoya University, Nagoya, Japan, 1990).
- 4) H. Pagels and S. Stokar, Phys. Rev. **D20** (1979), 2947.
- 5) W. A. Bardeen, C. T. Hill and M. Lindner, Phys. Rev. **D41** (1990), 1647.
- 6) T. Eguchi, Phys. Rev. **D14** (1976), 2755.
- 7) K. Yamawaki, in *Proc. Workshop on Effective Field Theories of the Standard Model, Dobogókő, Hungary, August 22-26, 1991*, ed. U.-G. Meissner (World Scientific Pub. Co., Singapore, 1992), p. 307.  
M. Tanabashi, in *Proc. Int. Workshop on Electroweak Symmetry Breaking, Hiroshima, November 12-15, 1991*, ed. W. A. Bardeen, J. Kodaira and T. Muta (World Scientific Pub. Co., Singapore, 1992), p. 75.
- 8) K. Yamawaki, Prog. Theor. Physics. Suppl. No. 123 (1996), 19.  
I. Inukai, M. Tanabashi and K. Yamawaki, in *Proc. of 1996 Int. Workshop on Perspectives of Strong Coupling Gauge Theories (SCGT '96), Nagoya, Nov. 13-16, 1996*, ed. J. Nishimura and K. Yamawaki (World Scientific Pub. Co., Singapore, 1997), p. 44.
- 9) L. Lavoura, Int. J. Mod. Phys. **A7** (1992), 3593.  
W. T. A. ter Veldhuis, Phys. Rev. **D45** (1992) 3201.
- 10) T. Appelquist, J. Terning and L. C. R. Wijewardhana, Phys. Rev. **D44** (1991), 871.
- 11) V. A. Miransky and K. Yamawaki, Mod. Phys. Lett. **A4** (1989), 129.  
K.-I. Kondo, S. Shuto and K. Yamawaki, Mod. Phys. Lett. **A6** (1991), 3385.
- 12) H. Georgi, E. H. Simmons and A. G. Cohen, Phys. Lett. **B236** (1990), 183.  
T. Kugo and M. G. Mitchard, Phys. Lett. **B282** (1992), 162.  
E. H. Simmons, Phys. Rev. **D42** (1990), 2933.  
K.-I. Kondo, T. Ebihara, T. Iizuka and E. Tanaka, Nucl. Phys. **B434** (1995), 85.
- 13) W. A. Bardeen, C. N. Leung and S. T. Love, Phys. Rev. Lett. **56** (1986), 1230.  
C. N. Leung, S. T. Love and W. A. Bardeen, Nucl. Phys. **B273** (1986), 649.
- 14) K.-I. Kondo, H. Mino and K. Yamawaki, Phys. Rev. **D39** (1989), 2430.  
K. Yamawaki, in *Proc. Johns Hopkins Workshop on Current Problems in Particle Theory*

- 12, Baltimore, June 8-10, 1988*, ed. G. Domokos and S. Kovesi-Domokos (World Scientific Pub. Co., Singapore, 1988).
- T. Appelquist, M. Soldate, T. Takeuchi and L. C. R. Wijewardhana, *ibid.*
- 15) J. M. Cornwall, R. Jackiw and E. Tomboulis, *Phys. Rev.* **D10** (1974), 2428.  
For a recent review, R. W. Haymaker, *Riv. Nuovo Cim.* **14** (1991), 1.
- 16) See, for example, V. A. Miransky, *Dynamical Symmetry Breaking in Quantum Field Theories* (World Scientific Pub. Co., Singapore, 1993).
- 17) V. A. Miransky, *Sov. J. Nucl. Phys.* **38** (1983), 280.  
K. Higashijima, *Phys. Rev.* **D29** (1984), 1228.
- 18) K.-I. Kondo, M. Tanabashi and K. Yamawaki, unpublished (1993).
- 19) D. Atkinson, *J. Math. Phys.* **28** (1987), 2494.
- 20) W. J. Marciano, *Phys. Rev. Lett.* **62** (1989), 2793; *Phys. Rev.* **D41** (1990), 219.
- 21) Shen Kun and Q. Zhongping, *Phys. Rev.* **D45** (1992), 3877.  
K. Shen and Y. P. Kuang, *Phys. Rev.* **D57** (1998), 6386.  
M. Hashimoto, hep-th/9805035.
- 22) M. Hashimoto, T. Ito, S. Nishiguchi and K. Yamawaki, in preparation.
- 23) G. Cvetič and N. D. Vlachos, *Phys. Lett.* **B377** (1996), 102.
- 24) V. P. Gusynin and M. Reenders, *Phys. Rev.* **D57** (1998), 6356.